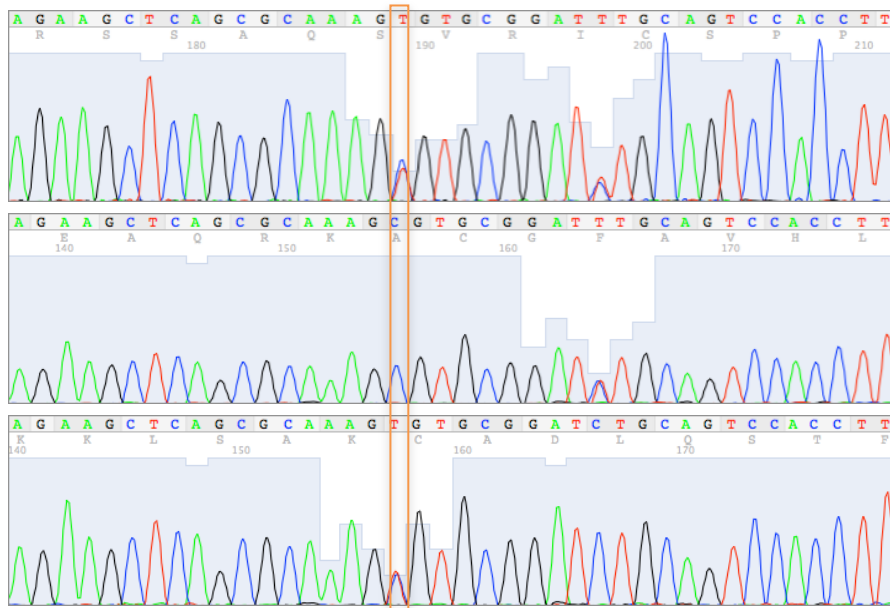


Supplemental Figure 1

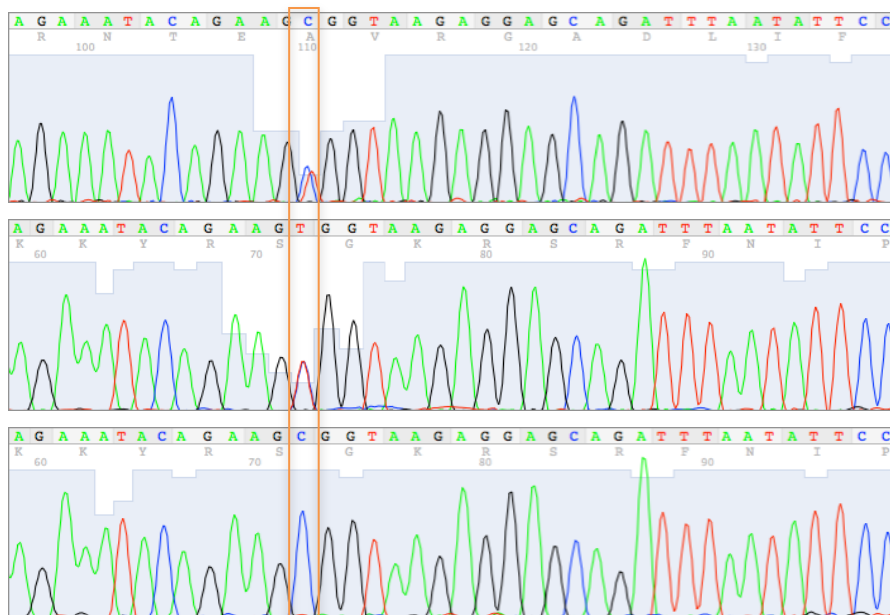
MCM10:Chr10:13230941_C>T:exon10:c.1276C>T:p.R426C

Proband: C>T
[C/T]

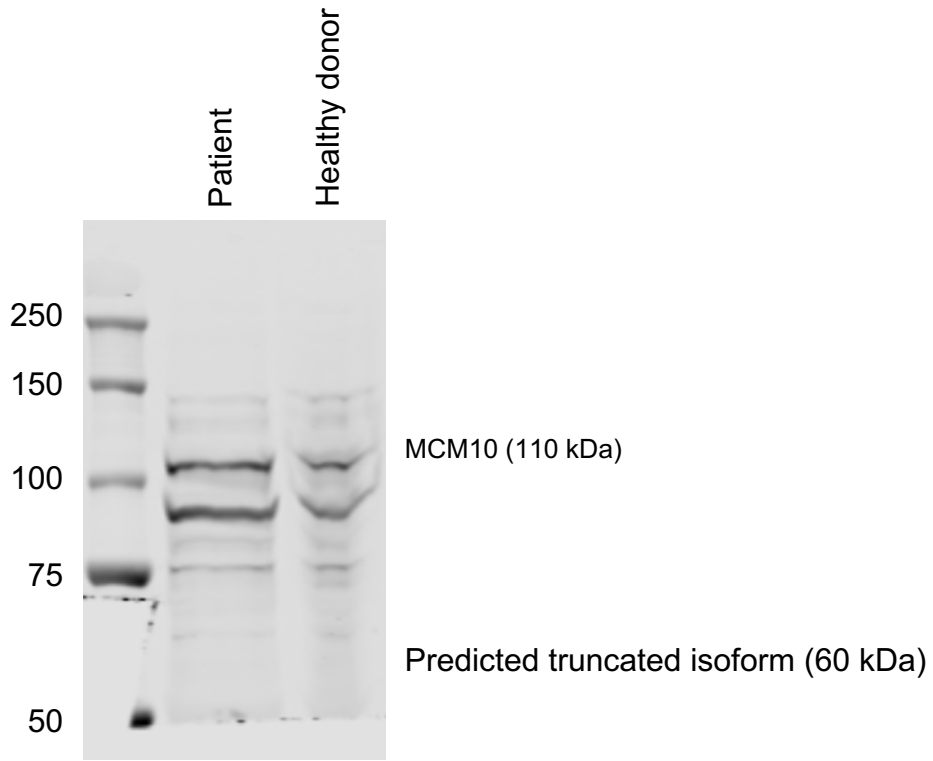


MCM10:Chr10:13234567_C>T:exon13:c.1744C>T:p.R582X

Proband: C>T
[C/T]



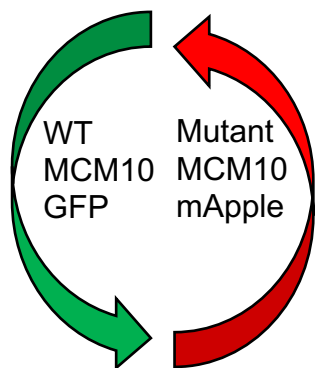
Supplemental Fig. 2



Supplemental Fig 3.

A

pBABE retroviral vector



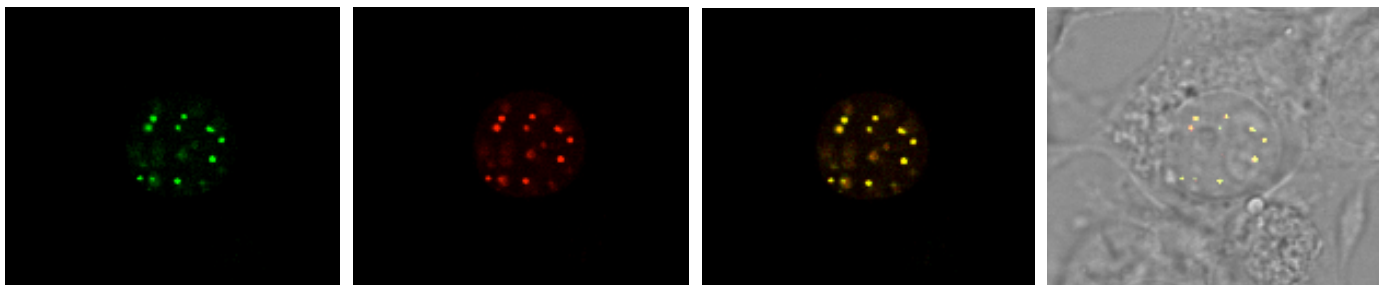
B

GFP (C1276)

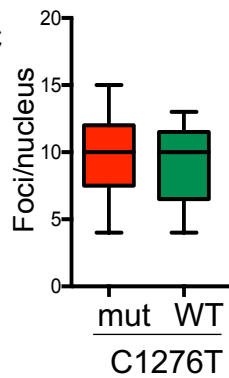
mApple (C1276T)

Merge

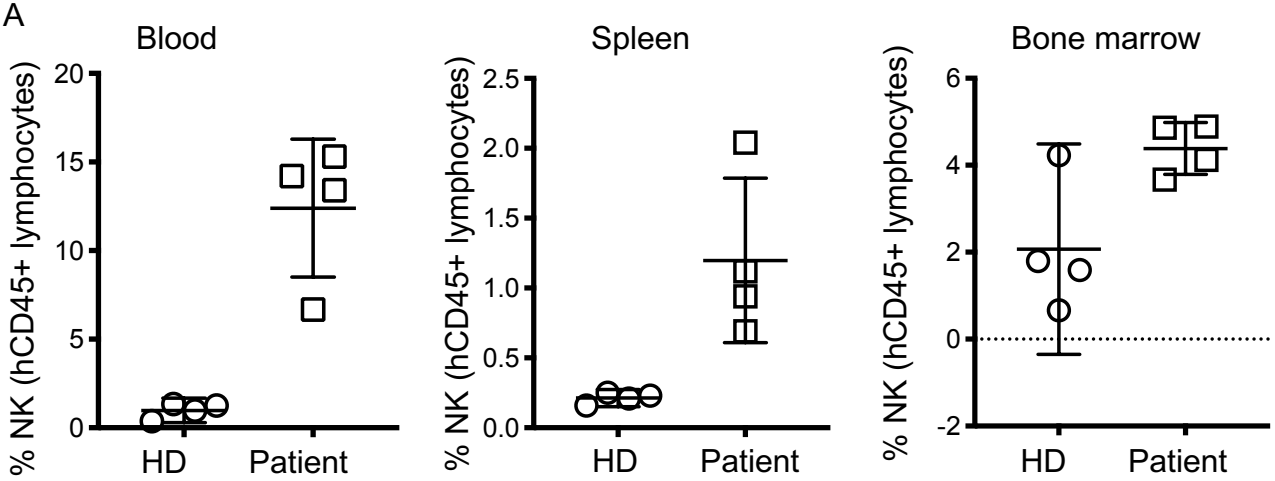
Merge (DIC)



C



Supplemental Fig. 4



Supplemental Material

Supplemental Figure 1. Sanger sequencing confirmation of c.1276C>T and c.1744C>T nucleotide variants in the patient and his parents (GRCh37/hg19).

Supplemental Figure 2. Western blot for MCM10 using full-length polyclonal immunogen. A) Primary fibroblasts from the proband and a healthy donor were lysed and probed for MCM10 protein (left) using polyclonal antibody raised against full-length MCM10. Predicted MW of truncated isoform=60 kDa.

Supplemental Figure 3. Bicistronic WT/R426C vector. A) Schematic of pBABE vector expressing full-length WT MCM10 with a GFP reporter, and MCM10 R426C with an mApple reporter. B) Transient transfection of the bicistronic vector in Phoenix cells followed by live cell imaging. C) Fluorescent foci per nucleus were enumerated using FIJI.

Supplemental Figure 4. Frequency of NK cells from mice reconstituted with CD34⁺ cells derived from iPSCs. iPSCs reprogrammed from patient primary fibroblasts were differentiated by teratoma formation to CD34⁺ HSC then purified and transplanted into NSG mice. Organs were harvested 21 days following transplantation. A) Frequency of NK cells within the human CD45⁺ gate as indicated. n=4 mice per genotype (patient and healthy donor derived iPSCs). Mean±95% CI.

Chromosomal coordinates (hg19)	Coding change	Protein change	Zygoty	Mat/Pat	Type	BHCMG exomes	gnomAD exomes	gnomAD genomes	CADD v1.3	pLI
Homozygous/hemizygous										
X:108638614_C>T	c.G2380A	p.E794K	Hemi	Mat	Nonsynonymous	0.003	0.004	0.004	33	0.000015
X:153224783_G>A	c.C1604T	p.T535M	Hemi	Mat	Nonsynonymous	0.00009	0	0	29.3	0.999996
Compound heterozygous										
16:70517824_G>T	c.C1759A	p.Q587K	Het	Pat	Nonsynonymous	0.004	0.005	0.004	9.303	4.39x10 ⁻⁶
16:70530308_A>G	c.T1508C	p.M503T	Het	Mat	Nonsynonymous	0.00009	0	0	12.82	4.39x10 ⁻⁶
2:186656179_C>G	c.C4583G	p.T1528R	Het	DN	Nonsynonymous	0.002	0.004	0.004	24.4	3.22x10 ⁻⁸
2:186664684_A>G	c.A10918G	p.I3640V	Het	Pat	Nonsynonymous	0.0003	0.0003	0.0001	5.791	3.22x10 ⁻⁸
14:31792894_G>A	c.C2785T	p.R929X	Het	Pat	Stopgain	0.0002	0.000008	0.00003	39	NA
14:31806781_C>T	c.G2389A	p.V797I	Het	Mat	Nonsynonymous	0.0006	0.0005	0.0008	23.5	NA
1:152188862_G>A	c.C5243T	p.S1748L	Het	DN	Nonsynonymous	0.0005	0	0.00007	9.724	5.01x10 ⁻²⁹
1:152191686_A>C	c.T2419G	p.Y807D	Het	Pat	Nonsynonymous	0.0002	0.00009	0.00006	0.046	5.01x10 ⁻²⁹
10:13230941_C>T	c.C1276T	p.R426C	Het	Pat	Nonsynonymous	0.0001	0.00002	0.00006	28.5	5.09x10 ⁻¹¹
10:13234567_C>T	c.C1744T	p.R582X	Het	Mat	Stopgain	0.00009	0	0	37	5.09x10 ⁻¹¹
12:110348956_C>T	c.C968T	p.A323V	Het	Pat	Nonsynonymous	0.00009	0	0	27	7.00x10 ⁻¹²
12:110348977_A>G	c.A989G	p.Q330R	Het	Mat	Nonsynonymous	0.00009	0	0	12.67	7.00x10 ⁻¹²
Heterozygous, inherited										
1:207653397_C>T	c.C3187T	p.R1063C	Het	Pat	Nonsynonymous	0.0005	0.0005	0.0003	32	2.17x10 ⁻¹¹
5:137897266_T>C	c.1182+3A>G		Het	Mat	Splicing	0.0002	0.0002	0.00003	NA	0.981119
21:46308800_C>T	c.G1888A	p.E630K	Het	Mat	Nonsynonymous	0.003	0.005	0.005	29.6	3.88x10 ⁻⁵
22:36745275_G>C	c.C7G	p.Q3E	Het	Mat	Nonsynonymous	0.002	0.002	0.002	13.5	1
16:50745853_C>G	c.C2031G	p.F677L	Het	Pat	Nonsynonymous	0.0001	0.00003	0.00006	26.1	5.52x10 ⁻¹⁹
7:82997128_C>A	c.G2102T	p.S701I	Het	Mat	Nonsynonymous	0.006	0.005	0.002	8.216	0.030448
16:3640271_G>T	c.C3368A	p.S1123Y	Het	Pat	Nonsynonymous	0.0003	0.0003	0.0003	25.4	8.90x10 ⁻⁸
2:217293430_T>C	c.T1259C	p.V420A	Het	Pat	Nonsynonymous	0.0003	0.0001	0.00003	16.65	0.000314
Heterozygous, de novo										
1:152275799_T>C	c.A11563G	p.R3855G	Het	DN	Nonsynonymous	0.00004	0	0	0.004	NA
5:110456695_T>C	c.T2172C	p.D724D	Het	DN	Cryptic splicing	0.00004	0	0	NA	0.544024

Supplementary Table 1: Candidate variants identified by exome sequencing and filtered for rare variants as described in Methods and Ref. 33A.

Additional Supplemental Methods

Exome sequencing and analysis

Exonic portions of genomic DNA were captured with custom VCrome probes (52 Mb; Roche NimbleGen Inc.) and DNA was sequenced using Illumina HiSeq 2500 equipment (Illumina). Sample preparation, capture method, sequencing, bioinformatic processing, filtering and the gene variant databases used, and further manual evaluation and interpretation of the exome data have previously been published in detail (1).

The initial exome analysis was performed at a time when the normal variant databases such as ESP5400 (<http://evs.gs.washington.edu/EVS>), 1000 genomes (2), and our in-house laboratory database (3) contained less than 10,000 sequenced individuals. Reanalyzing the three exomes annotated to present gene variant databases such as gnomAD (4), and filtering on minor allele frequency of less than 0.0005 in the updated in-house database at Baylor Hopkins Center for Mendelian Genomics (BHCMG, <http://bhcmg.org/>), supports the selection of the compound heterozygous MCM10 variants in the proband's sequence file. Based on the prediction tool Combined Annotation Dependent Deletion (CADD) (5) the two *MCM10* variants receive a high score as compared to the other variants (Supplementary Table 1).

Cell lines

293T S-protein tag, Flag tag, Streptavidin binding peptide (SFB)-MCM10 stable cell lines were grown in DMEM (Gibco 11995) supplemented with 10% FBS (Sigma F4135), 1% penicillin/streptomycin (Gibco 15140) at 37°C and 5% CO₂. Immortalized retinal

pigmented epithelial cells (hTERT-RPE-1) were grown in DMEM:F12 supplemented with 10% FBS (Sigma F4135), 1% penicillin/streptomycin (Gibco 15140) at 37°C and 5% CO₂. To generate a homozygous cell line for the R426C exon10 patient variant, a guide RNA targeting exon 10 of *MCM10* and a single stranded oligo containing the desired point mutation were transfected into hTERT RPE-1. Cells were then subcloned and individual clones were screened for targeting. Biallelic knock-in of the mutation was confirmed with sequencing of TOPO TA clones. In a similar manner, heterozygous R582X (exon 13) patient *MCM10* variant cell lines were generated using a guide RNA to the intronic region adjacent to the mutation location. A plasmid containing the point mutation and flanking regions of homology was used as a donor molecule to insert the patient *MCM10* variant. Cells were then subcloned and individual clones were screened for targeting. Biallelic knock-in of the mutation was confirmed with sequencing of TOPO TA clones.

CRISPR-edited NK cells were generated by nucleofecting NK92 cells or CD34⁺ precursors with pCMV-Cas9-GFP all-in-one plasmid (Sigma-Aldrich) with the intronic guide sequence GAT TTA ATA TTC CCC GCT TGG G. Single cell clones were isolated by FACS sorting for GFP positive clones and expanded in culture. *MCM10* knockdown was measured by Western blot and quantitative PCR. Primary patient or healthy donor fibroblasts were immortalized by lentiviral transduction with SV40 large T antigen transformation, selected with puromycin and confirmed by PCR for SV40 expression (Applied Stemcell). 293T fibroblast lines were maintained in DMEM supplemented with 10% FBS, penicillin/streptomycin, L-glutamine and sodium pyruvate. Transient transfections of wild-type or mutated *MCM10*-expressing plasmids were performed by

transfecting 2×10^6 cells with 6 μg of DNA using Lipofectamine 2000 according to manufacturers' instructions (Invitrogen).

Western blots

Immortalized fibroblasts from patient or healthy donor were lysed in RIPA buffer supplemented with Halt proteinase phosphatase (Pierce). For nuclear and cytoplasmic fractionation, cells were lysed in cytosolic buffer (10mM HEPES pH8, 10mM KCl, 1mM EDTA pH 8, 0.4% NP40, 1X Halt proteinase phosphatase) and nuclear buffer (20mM HEPES pH 8, 450mM NaCl, 1mM EDTA pH 8, 1X Halt proteinase phosphatase). For co-immunoprecipitation of chromatin-associated proteins, 293T cells transiently transfected with p-Lenti turboGFP MCM10 plasmids were lysed in cytosolic buffer as described above, then the nuclear pellet was resuspended in co-IP buffer (10mM Tris-HCl pH7.5, 150mM NaCl, 0.5M EDTA, 0.5% NP40, 1X Halt proteinase phosphatase inhibitor) supplemented with 75U/ml DNase I and 2.5mM MgCl_2 for 30' at 4°C. Lysates were incubated with anti-turboGFP antibody (mouse monoclonal OTI2H8, TA150041, Origene) or IgG isotype (NCG2B.01, Invitrogen) and Dynabeads Protein G (Invitrogen). Lysates for co-IP of CDC45 and MCM2 were incubated with turbo-GFP trap_MA antibody (Chromotek) or control binding antibody (bmab-20, Chromotek). For tight chromatin fractionation, cell pellets were subsequently washed in cytosolic buffer and nuclear buffer as described above and 50mM Tris-HCl pH8, 0.05% NP-40 buffers with increasing concentration of NaCl (0.15, 0.30M). Lysates were separated by gradient 4-12% gel and transferred to nitrocellulose membrane. Membranes were blocked using skim milk. Western blotting was performed using antibodies against the following:

MCM10 (rabbit polyclonal, 12251-AP, Proteintech), MCM2 (rabbit polyclonal, ab4461, Abcam), CDC45 (rabbit monoclonal D7G6, 11881S, Cell Signaling Technologies), POLA (rabbit polyclonal, ab176734, Abcam), PCNA (rabbit polyclonal, ab18197, Abcam), lamin B1 (rabbit polyclonal, ab16048, Abcam), α -tubulin (mouse monoclonal DM1A, T9026, Sigma); actin (rabbit polyclonal, A5060, Sigma). Secondary detection was performed using near-infrared dye (IRDye) goat anti-Rabbit (Licor 926-32211) or goat anti-mouse light chain specific (Licor, 115-625-174) antibodies which were visualized by LiCor Odyssey and protein intensity was normalized to loading controls using ImageJ software.

For 293T SFB-MCM10 stable cell lines, whole cell extracts were prepared as previously described (6) and analyzed with the following antibodies in 5% BLOT-QuickBlocker (G-Biosciences 786-011) in TBST: anti-FLAG antibody (Sigma F3165; 1:500 overnight at 4°C) and anti- α -Tubulin (Covance MMS407R ; 1:20,000 overnight at 4°C). Detection was with WesternBright Quantum detection kit (K-12042-D20).

For hTERT RPE-1 mutant cells, whole cell extracts were prepared as previously described (6) and analyzed with the following antibodies in 5% BLOT-QuickBlocker (G-Biosciences 786-011) in TBST: anti-MCM10 (Novus Biologicals H00055388-D01P; 1:500 overnight at 4°C) which is a polyclonal antibody that was raised to full length MCM10 allowing detection of truncated protein, anti-MCM10 (Bethyl A300-131A; 1:500 overnight at 4°C) which was raised to an epitope in the C-terminal domain of MCM10, and tubulin (anti- α -tubulin, Covance MMS407R ; 1:20,000 overnight at 4°C). Proteins were detected with WesternBright Quantum detection kit (K-12042-D20).

Microscopy and image analysis

For preparation of microscopy samples, patient fibroblasts or transiently transfected cell lines were introduced into #1.0 Biotek imaging chambers and allowed to adhere overnight. For stably transfected cell lines or primary cells from NSG mice, cells were incubated for 30 minutes on #1.5 coverslips previously coated with poly-L-lysine (Sigma-Aldrich). Cells were fixed and permeabilized (Cytifix/Cytoperm, BD Biosciences) and incubated with polyclonal anti-MCM10 antibody (Abcam) followed by goat anti-rabbit secondary antibody conjugated to Alexa Fluor 488 (ThermoFisher). Cells were alternatively incubated with anti- γ H2AX antibody directly conjugated to Alexa Fluor 647 or Alexa Fluor 488 (2F3, Biolegend) and anti-fade mounting media containing DAPI was added to the wells. For visualization of 293T cells transiently expressing GFP-containing vectors and patient mutations, cells were grown in 8 well chamber slides with removable chambers for 24-48 hours after transfection. At this time, cells were fixed and permeabilized, then chambers were removed and coverslips were mounted with ProLong Gold antifade with DAPI (Thermo Fisher).

Images were acquired on a Leica SP8 confocal microscope equipped with a 100X 1.45 NA objective, with excitation by tunable white light laser. Detection was by HyD detectors and images were acquired with LASAF software. For some experiments, images were acquired on a Zeiss Axioplan Observer Z1 with Yokigawa CSU-10 spinning disk and 63X 1.49 NA objective. Excitation was by 405 nm, 488 nm, 561 nm and 637 nm Coherent OBIS LX lasers controlled by a MultiLine Laserbank and controller (Cairn) and images were recorded with a Hamamatsu Orca R2 camera. Data were acquired by MetaMorph. After acquisition, all data were exported and analyses

were performed in Fiji (7). For measurement of nuclear size, area of DAPI staining was ascertained. For measurement of nuclear MCM10 or GFP intensity, nuclei were segmented using DAPI and the intensity of MCM10 or GFP above negative control was quantified for each nucleus. For measurement of γ H2AX, the intensity and area of signal above negative control were measured. Data were graphed and statistical analyses performed in Prism 6.0 (GraphPad Software).

For 293T SFB-MCM10 stable cell lines, cells were plated on Millicell EZ slides (Millipore PEZGS0416) and allowed to recover for 24 hours. Cells were fixed with 3% paraformaldehyde in 1xPBS for 15 minutes and then permeabilized with 0.5% Triton-X-100 in 1xPBS for 5 minutes. Cells were stained with primary anti-FLAG antibody (Sigma F3165; 1:500) for 30 minutes at 37°C, followed by secondary anti-mouse Alexa Fluor 488 (ab150113), DAPI staining, and mounted using Vectashield (Vector Laboratories H-1000). Images were acquired using an Olympus FluoView FV1000 IX2 Inverted Confocal (University Imaging Centers at the University of Minnesota) and processed using FIJI and Adobe Photoshop.

For hTERT RPE-1 mutant cell lines, cells were plated on #1.5 coverslips and allowed to recover for 24 hrs. Cells were then washed with PBS and treated with 20J UV and media replaced. For those cells that were untreated, they were washed with PBS and had fresh media immediately replaced. Cells were allowed to recover for 24 hours before being fixed in 3% paraformaldehyde in 1X PBS for 10 minutes and then permeabilized with 0.5% Triton-X-100 in 1xPBS for 5 minutes. Cells were blocked for 1 hour at room temperature in ABDIL (20mM Tris pH 7.5, 2% BSA, 0.2% fish gelatin, 130mM NaCl) followed by staining with primary anti- γ H2AX (Bethyl A300-081A) in

ABDIL overnight at 4°C. They were then washed 3 times in PBST (1x PBS and 0.1% Tween) before staining with secondary anti-rabbit Alexa Fluor 488 (Thermo Fisher) for 1 hour at room temperature. Coverslips were washed 3 times in PBST, where the second wash contained DAPI, and mounted using Vectashield (Vector Laboratories H-1000). Slides were imaged on a Zeiss spinning disc confocal microscope using 100X 1.45 NA objective and 405nm and 488nm lasers. For image analysis FIJI was used to flatten images from both channels. After datasets were blinded, points with local maximal intensity were identified using FIJI and counted for each nucleus. Statistical analysis and graphical representation were performed in Prism 8.4.1.

Flow cytometry of in vitro derived NK cells

Subsets were quantified using previously described phenotypic markers that mark progression from Stage 1 (CD34⁺ CD117⁻ CD94⁻CD16⁻) through Stage 2 (CD34⁺CD117⁺CD94⁻CD16⁻), then Stage 3 (CD34⁻CD117⁺CD94⁻CD16⁻), Stage 4 (CD34⁻CD117^{+/-}CD94⁺CD16⁻) and Stage 5 (CD34⁻CD117⁻CD94^{+/-}CD16⁺) (8). Flow cytometry was performed with the following antibodies: CD57 (Pacific Blue, clone HCD57, Becton Dickinson), CD56 (Brilliant Violet 605, clone HCD56, Biolegend), CD3 (Brilliant Violet 711, clone SK7, Biolegend), CD62L (Brilliant Violet 655, DREG56, Biolegend), CD16 (PE Texas Red, clone 3G8, BD Biosciences), CD94 (APC, DX22, Biolegend), CD34 (PE, 4H11, eBiosciences), and CD117 (PE Cy7, 104D2D1, Beckman Coulter). Flow cytometry data were acquired on a BD Fortessa analyzer and exported to FlowJo (Treestar Inc.) for further analyses.

Validation of iPSCs

Newly derived iPSCs were passaged at least three times before banking. Cell lines were evaluated by karyotype analysis using G-banded karyotyping. They were further characterized for expression of pluripotency genes using qPCR (REX1, SOX2, NANOG and HTERT) and immunofluorescence (TRA-1-60 (Millipore; MAB4360), SSEA-3 (Millipore; MAB4303), SSEA-4 (Millipore; MAB4304), NANOG (Abcam; ab21624) and OCT4 (Abcam; ab19857). Lastly iPSC lines were differentiated in a spontaneous differentiation assay and expression of markers of three germ layers was assessed using qPCR for GATA4, AFP, CTnT, FLK1, PAX6, TUBB3, BRA and TUJ1. They were further characterized by karyotype analysis, expression of pluripotency genes and differentiation genes in a spontaneous differentiation assay. RNA was extracted using RNeasy Mini-Kit (Qiagen) and complementary DNA synthesized using KAPA cDNA Mix. iPSCs were maintained on Matrigel in mTESR media at 37°C/5% CO₂.

Human CD34⁺ HSC magnetic column purification and reconstitution of NSG mice

A 1 mg/mL solution of collagenase/dispase (Sigma) was prepared and injected into multiple points of teratomas to ensure penetration into the tissue. Teratomas were then minced into 1-mm pieces and poured into 15-mL conical tubes with approximately 10 mL of collagenase/dispase enzyme solution per teratoma. The tubes were incubated for 90 minutes at 37°C on a platform agitator. After incubation, the teratomas were filtered three times through 70 µM nylon mesh and washed with PBS + 2% FBS. The teratoma cell suspension was then poured onto a Ficoll gradient and centrifuged for 20 minutes, 300g at room temperature. The cell layer was extracted and counted to prepare for

magnetic column purification. A Miltenyi Biotec MACS CD34 MicroBead kit was used to positively select hematopoietic stem cells from teratoma single cell suspension after magnetic column purification. Cell suspensions were incubated for thirty minutes at 4°C with FcR blocking reagent and magnetic microbeads bound to anti-human CD34 antibodies. The solution was then applied to a positive selection column, which was held in place by a magnet. Buffer containing PBS, 0.5% bovine serum albumin, and 2 mM EDTA was used to flush columns. The column flowthrough was discarded, and the eluent was applied to a second column to increase purity. The final eluent was counted and a small aliquot was used to check percent purity of HSCs via flow cytometry. Purity was measured as percent of CD34+ cells out of total cells and was generally above 97%. The cells were then washed and resuspended in PBS + 2% FBS to achieve a final concentration of 50,000 HSCs per 20 μ L. Previously irradiated one-day-old pups were injected intrahepatically with 50,000 HSCs, and were monitored routinely for survival and development of graft versus host disease.

Isolation of immune cells from humanized mice and flow cytometric analysis

Blood: Heart bleeds with a syringe were performed on mice immediately after death. Blood was collected in a FACS tube containing approximately 500 μ L PBS + heparin. Blood samples were diluted 1:1 with PBS and layered over a Ficoll gradient. The gradients were centrifuged for 20 minutes, 300g at room temperature. The cell layer was extracted and counted to prepare for flow cytometry staining.

Spleen: Frosted slides were used to disaggregate the spleens into a solution of PBS + 2% FBS. Cells were filtered through 40 μ M nylon mesh and centrifuged for 5 minutes,

300g at room temperature. Red Blood Cells were lysed using Ammonium-Chloride-Potassium buffer for 2 minutes followed by washing of the cells with PBS + 2% FBS and centrifugation for 5 minutes, 300g at room temperature. The volume was brought to a convenient mark for counting, and the cells were counted to prepare for flow cytometry staining.

Bone marrow: Right and left tibias and femurs were removed from mice during dissection. A syringe loaded with PBS + 2% FBS was used to flush out the bone marrow. This solution was filtered through 40 μ M nylon mesh and centrifuged for 5 minutes, 300g at room temperature. The volume was brought to a convenient mark for counting, and the cells were counted to prepare for flow cytometry staining.

Freshly isolated cells were stained for flow cytometry using the following antibodies: CD57 (Pacific Blue, clone HCD57, Becton Dickinson), CD56 (Brilliant Violet 605, clone HCD56, Biolegend), CD45 (PE-Cy5, HI30, Biolegend), CD3 (Brilliant Violet 711, clone SK7, Biolegend), CD62L (Brilliant Violet 655, DREG56, Biolegend), CD16 (PE Texas Red, clone 3G8, BD Biosciences), CD94 (APC, DX22, Biolegend), CD34 (PE, 4H11, eBiosciences), CD117 (PE Cy7, 104D2D1, Beckman Coulter). Incubation with antibody was performed on ice for 30 minutes prior to washing with PBS 2% FCS. Compensation controls were prepared using single stained OneComp beads (BD Biosciences). Fluorescence minus one controls were additionally prepared for CD45 and CD56 with splenocytes. Data were acquired on a BD Fortessa and analyzed in FlowJo (TreeStar). Approximately 10^6 events were recorded from each organ from 4 mice per genotype.

Statistics

Data were tested for normality using D'Agostino & Pearson or Shapiro-Wilk tests. Single comparisons with normal distribution were analyzed by two-tailed student's T-test and those containing data that were not normally distributed were analyzed by two-tailed Mann-Whitney test. For data comparing test data to a defined value, such as normalized data comparing to a wild-type condition normalized to 1, data were tested with a one sample t and Wilcoxon test. For multiple comparisons with data normally distributed, one-way ANOVA with corrections was performed. For multiple comparisons containing data not normally distributed Kruskal-Wallis tests with Dunn's correction were performed. Where technical replicates or representative datasets are shown, such as repeated testing of cell lines, replicate experiments were performed on independent days. All statistical analyses were performed in Prism 6.0, 7.0 or 8.0 (GraphPad Software). Values were considered statistically non-significant when $P > 0.05$. P values are represented on graphs as statistically significant as follows: * $P \leq 0.05$, ** $P \leq 0.01$, *** $P \leq 0.001$, **** $P \leq 0.0001$.

References

1. Stray-Pedersen A, Sorte HS, Samarakoon P, Gambin T, Chinn IK, Coban Akdemir ZH, et al. Primary immunodeficiency diseases: Genomic approaches delineate heterogeneous Mendelian disorders. *J Allergy Clin Immunol*. 2017;139(1):232-45.
2. Genomes Project C, Abecasis GR, Altshuler D, Auton A, Brooks LD, Durbin RM, et al. A map of human genome variation from population-scale sequencing. *Nature*. 2010;467(7319):1061-73.
3. Yang Y, Muzny DM, Reid JG, Bainbridge MN, Willis A, Ward PA, et al. Clinical whole-exome sequencing for the diagnosis of mendelian disorders. *N Engl J Med*. 2013;369(16):1502-11.
4. Karczewski KJ, Francioli LC, Tiao G, Cummings BB, Alföldi J, Wang Q, et al. Variation across 141,456 human exomes and genomes reveals the spectrum of loss-of-function intolerance across human protein-coding genes. *bioRxiv*. 2019:531210.
5. Kircher M, Witten DM, Jain P, O'Roak BJ, Cooper GM, and Shendure J. A general framework for estimating the relative pathogenicity of human genetic variants. *Nat Genet*. 2014;46(3):310-5.
6. Becker JR, Gallo D, Leung W, Croissant T, Thu YM, Nguyen HD, et al. Flap endonuclease overexpression drives genome instability and DNA damage hypersensitivity in a PCNA-dependent manner. *Nucleic Acids Res*. 2018;46(11):5634-50.
7. Schindelin J, Arganda-Carreras I, Frise E, Kaynig V, Longair M, Pietzsch T, et al. Fiji: an open-source platform for biological-image analysis. *Nat Methods*. 2012;9(7):676-82.
8. Freud AG, Yokohama A, Becknell B, Lee MT, Mao HC, Ferketich AK, et al. Evidence for discrete stages of human natural killer cell differentiation in vivo. *J Exp Med*. 2006;203(4):1033-43.